

## Fluorescence in nanostructured fulleride films

R. F. M. Lobo,<sup>a)</sup> M. S. Costa, J. H. F. Ribeiro, C. A. C. Sequeira, and P. Pereira

*Grupo de Nanotecnologia e Ciência à Nano-Escala, Faculdade de Ciências e Tecnologia da Universidade Nova de Lisboa, 2829-516 Caparica, Portugal and Instituto Ciência e Engenharia de Materiais e Superfícies (ICEMS), Av. Rovisco Pais, IST, 1049-001 Lisboa, Portugal*

(Received 8 July 2006; accepted 7 September 2006; published online 13 November 2006)

Nanostructuring of fullerene C<sub>60</sub> beam deposited films is achieved by electrochemical reduction in a potassium hydroxide aqueous solution. Alkali fulleride clusters are formed at the electrode, as it is illustrated by cyclic voltammetry, x-ray diffraction, and scanning tunneling microscopy. Fluorescence emission from fluorophore doped fullerene reduced films was investigated by fluorescence spectroscopy and scanning near-field optical microscopy. These techniques lead to results which also fit such nanometer-sized fulleride cluster interpretation. In particular, the fluorophore fluorescence lifetime decreases as long as aggregation in the film is more effective, which occurs with the increase of film thickness. © 2006 American Institute of Physics. [DOI: 10.1063/1.2388245]

There is current great interest in the possible use of fullerene nanoclusters as suitable candidates for designing miniaturized electrodes with high-surface area and robust films on desired electrode surfaces with a well-controlled morphology.<sup>1,2</sup>

Despite the simple drop coating technique which enables the preparation of reasonable ordered fullerene films on substrates of highly oriented pyrolytic graphite (HOPG),<sup>3</sup> scanning probe microscopy studies have revealed nonuniformity in such films.<sup>4</sup> In addition, formation of high-quality Langmuir-Blodgett films of pure C<sub>60</sub> is difficult<sup>4,5</sup> because of the tendency of the buckyball Langmuir films to form multilayers and aggregates. On the contrary, adlayers prepared by sublimation in vacuum can reveal good uniformity.<sup>6</sup>

Neutral C<sub>60</sub> films are intrinsic semiconductors,<sup>7</sup> and their electrochemistry in various solvents deal with the production and properties of various salts of fullerenes, such as alkali fullerides. The electrochemical doping consists in the incorporation of cations during reduction for charge compensation. In nonaqueous solvents, where both C<sub>60</sub> and its anions are soluble, up to six electrons can be injected into the molecule by reversible charge-transfer reactions,<sup>8</sup> and the reduction of C<sub>60</sub> in toluene show that the process involves successive additions of electrons to the molecule.<sup>9</sup> Fullerene films can be reduced in aqueous solutions to produce salts with various counterions. The negligible solubility of the neutral and negative buckyballs in aqueous media allows the study of charge-transfer processes within the solid fullerene film.<sup>10</sup>

Our fullerene films are prepared in high vacuum by C<sub>60</sub> neutral beam deposition onto HOPG, and their thickness monitored through an appropriate quartz crystal microbalance.<sup>11,12</sup>

The prepared vapor-deposited C<sub>60</sub>/HOPG films, with thicknesses varying between 300 and 400 nm, have been used as electrodes in an electrolytical cell and immersed in a deaerated aqueous solution of 0.1M KOH. Voltammetry results are displayed in Fig. 1(a). The electrode was polarized from -200 to -1500 mV, yielding a sharp single cathodic current peak for the surface fullerene reduction. The peak

potential shifted gradually to -1600 mV with increasing thickness of the film due to the growing uncompensated film resistance. In the presence of K<sup>+</sup> ions, the reduction is accompanied by a voltammetric single peak and the reduction product is supposed to be the conducting K<sub>3</sub>C<sub>60</sub> salt. The absence of a reoxidation peak in the back scan of the voltammograms revealed an irreversible electron transfer to the C<sub>60</sub> molecules. According to the results, upon reduction of the C<sub>60</sub> nanocrystals, K<sup>+</sup> cations are incorporated into the fullerene film accompanied by a change in its structure to accommodate these counterions.<sup>11</sup>

Formerly hydrophobic, C<sub>60</sub> films become hydrophilic after reduction, and they have been monitored at the nanoscale using x-ray diffractometry and scanning tunneling microscopy (STM), operating at room pressure. The x-ray diffraction experiments obtained after electrochemical reduction [Fig. 1(b)] show a strong attenuation of the main diffraction peak (reflecting a change in the film structure), which occurs not only at the surface but in deeper fullerene layers as well. STM images of the dried 400 nm thick C<sub>60</sub> films deposited on HOPG before and after electrochemical reduction are displayed in Figs. 2(a) and 2(b). An ordered structure is revealed, where the distance between the C<sub>60</sub> molecules is close to 1 nm, in agreement with the x-ray diffraction measurements. Figure 2(b) shows the STM image of the fullerene upper layer (after reduction) for the thicker film (400 nm). No single buckyballs are detected, but instead clusters of probable K<sub>3</sub>C<sub>60</sub> molecules. The reduction is accompanied by a surface roughening enhancement factor of the order of 1.8.<sup>11</sup>

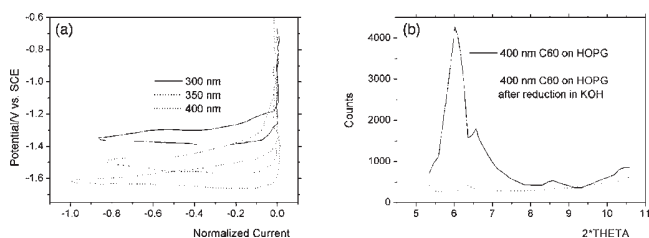


FIG. 1. (a) Voltammograms of a fullerene thin film electrode in a 0.1M KOH solution, at a potential scan rate of 500 mV/s, for three different thicknesses of the C<sub>60</sub> film. (b) X-ray diffraction plot of a 400 nm C<sub>60</sub> layer on HOPG before and after reduction in the 0.1M KOH solution.

<sup>a)</sup>Electronic mail: rfm@fct.unl.pt

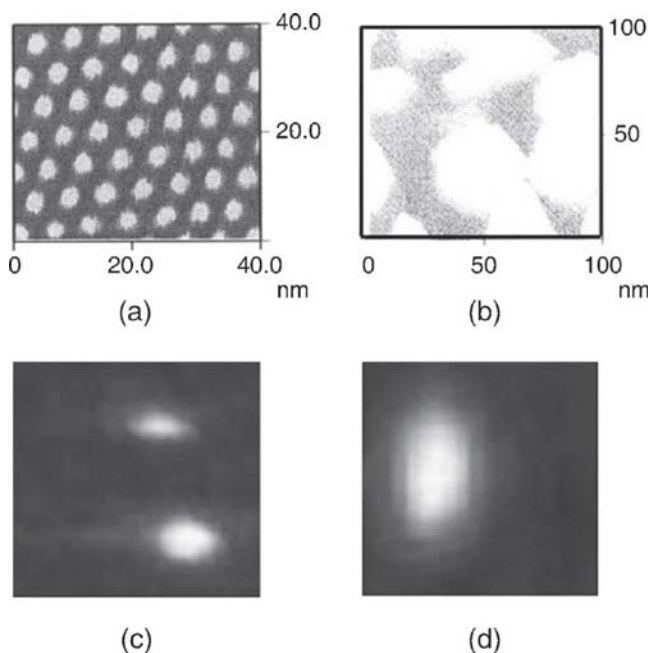


FIG. 2. Scanning probe images of  $C_{60}$  films (400 nm thick) deposited on HOPG: (a) STM image before electrochemical reduction, (b) STM image after electrochemical reduction in aqueous KOH solution, (c) fluorescence SNOM image before electrochemical reduction, and (d) fluorescence SNOM image after electrochemical reduction in aqueous KOH solution.

Scanning near-field optical microscopy (SNOM) combines the chemical sensitivity of optical spectroscopy techniques with the high spatial resolution of scanning probe microscopy and with the noninvasive character of light as well. Our SNOM instrument (Aurora Topometrix) provides highly correlated topography and optical images, and can be used to determine fluorescence spectra of individual nanoparticles or even molecules. The resolution in illumination mode is primarily limited by the size of the aperture and the aperture-sample distance. In addition, our SNOM has been improved with a homemade tuning fork resonance frequency automatic search. A graphical interface was developed in order to obtain an automatic procedure to find the resonant frequency of the tuning-fork probe. The signal processing between the SNOM and the tuning-fork probe is achieved with a lock-in phase sensitive signal detector/amplifier. The phase angle is used as a control signal for the proportional integral derivative. The lock-in interface allows us to perform a spectral scanning in a frequency range to be chosen by the user in order to find the exact probe resonance frequency. The automatic spectral scanning is only possible to perform if the controlling SNOM software (SPMLAB) is running in background mode in order to keep all the system in feedback. After inputting the value of the resonance frequency previously obtained, one could record topographic and optical reflection images for the same region of a standard calibration sample (Fig. 3).

In order to visualize nanostructures in the fullerene layers, the pristine coated HOPG electrodes were immersed in other KOH aqueous solutions, this time adding a fluorophore DiOC<sub>6</sub>(3) solution of 1.5  $\mu$ l (5 mg/ml in 100% of methanol) for 99  $\mu$ l of 0.1M KOH aqueous solution. The SNOM fluorescence images of the thicker film (400 nm), obtained before and after electrochemical reduction, are shown in Figs. 2(c) and 2(d).

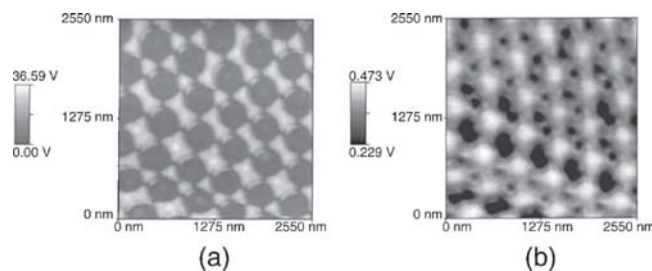


FIG. 3. (a) Standard sample topographic image and (b) standard sample optical image.

After using the above mentioned electrochemical fullerene reduction method, the dried films were spectroscopically analyzed with a UV-visible time fluorescence spectrometer. The excitation wavelength was supplied by a 628 nm  $Ar^+$  laser. With this wavelength one could assure a spectral isolation from Raman and fluorescence signals.

Figure 4(a) illustrates the fluorescence decay behavior observed with the thicker prepared film (400 nm) and in Fig. 4(b) one can observe the variation of the fluorescence decay time with the film thickness.

The fluorescence behavior of single macromolecules is dependent on their environment at the nanoscale.<sup>13</sup> The de-excitation decay for a single electron in an isolated fullerene molecule obeys a simple exponential law with a constant decay rate  $(\tau_F)^{-1}$  for all fullerenes. Assuming that at  $t=0$  s, the fluorescence quantum yield is  $\Phi(t)=(\tau_F)^{-1}N_0s(t)$  [where  $s(t)$  represents a fraction of excited fullerenes which remain in the emission state until the instant  $t$ ], one can determine such rate from the fluorescence decay curve by integration of the fluorescence rate between  $t=0$  and  $t \rightarrow \infty$ ,

$$(\tau_F)^{-1} = \eta / \langle \tau_{exc} \rangle, \quad (1)$$

where  $\eta = 1/N_0 \int \Phi(t) dt$  is the total fluorescence and  $\chi = \langle \tau_{exc} \rangle / \int s(t) dt$  the fullerene excited state lifetime. Deviations in fluorescence intensity are expected to arise from perturbations in the electronic structure of the molecules due to changes in the local environment.

The spectroscopic emission from DiOC<sub>6</sub>(3) embedded in fulleride films reveals a clear dependent deexcitation behavior on their thickness [Fig. 4(b)]. The fluorophore fluorescence lifetime decreases as long as aggregation in the film is more effective, which occurs with the increase of film thickness. The thicker films (with 400 nm) reveal an extremely fast deexcitation ( $\sim 10$  ps), compared with 1 ns observed for the solution of the fluorophore in methanol. This can be attributed to energy transfer among the fullerene clusters, which occurred with single-walled nanotube clusters.<sup>12,14</sup>

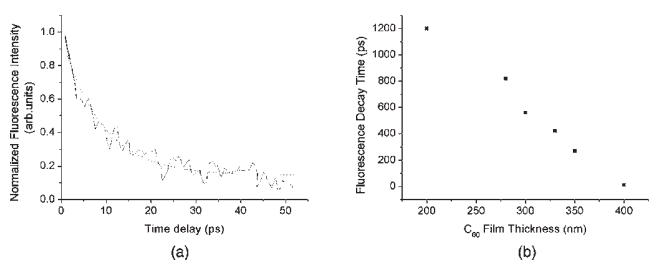


FIG. 4. (a) Fluorescence decay of  $C_{60}$  films (400 nm thick) deposited on HOPG. The dashed curve represents a first order exponential fit; (b) fluorescence lifetime vs fullerene film thickness.

Experimentally the following were obtained:  $\eta = 1.4 \times 10^{-4}$  and  $\langle \tau_{\text{exc}} \rangle = 12$  ps, which leads to  $\tau_F = 90$  ns for the fluorophore fluorescence lifetime.

In summary, electrochemical nanostructuring of fullerene layers on electrode surfaces by charge transfer has been achieved, and from the STM image of the fullerene upper layer obtained after the film reduction for the thicker film [Fig. 2(b)], no single buckyballs are detected, only clusters of probable  $K_3C_{60}$  molecules. In thicker films a significant change of film structure was observed. The injection of the first electron into a  $C_{60}$  molecule yields the  $C_{60}^-$  anion. The reaction is accompanied by an irreversible intercalation of  $K^+$  cations into the lattice of molecular fullerene crystals to compensate for the negative charge. The fullerene reduction was accompanied by an aggregation process in which clusters are likely to be formed.

The x-ray diffraction measurements of vacuum evaporated ultrathin buckyball films (tens of monolayers) usually display a typical fcc arrangement, with hexagonal pattern, and the layers with a (111) orientation have a lattice constant of about 1.4 nm, which is equal to a distance in fullerenes. This ordered structure is also clearly seen in our STM measurements, where the distance between the  $C_{60}$  molecules is close to 1 nm [Fig. 2(a)], in agreement with such x-ray diffraction experiments. STM images of thicker films usually present a more complicated picture, which have been interpreted by the formation of  $C_{60}$  clusters.<sup>15</sup> The SNOM image taken after electrochemical reduction of the thicker film [Fig. 2(d)] presents a broad unique fluorescence nanospot compared with the one obtained before reduction [Fig. 2(c)] which shows two smaller spots; this is likely to be a consequence of the fulleride clustering that creates more and larger vacancies filled with the fluorophore. In addition, the fluorophore fluorescence lifetime decreases as long as aggregation

in the film is more effective (which occurs with the increase of film thickness), and this can be attributed to energy transfer among the fullerene clusters.

Although the charge transfer mechanism could not be clarified, cooperation between electron hopping and ion diffusion is one real possibility. Furthermore, during electron transfer, the fullerene anions are likely to form C–C bonds and give rise to dimeric and even linear structures.

Support from FCT/MCTES is gratefully acknowledged.

- <sup>1</sup>Á. Szűcs, M. Tölgyesi, M. Csiszár, J. B. Nagy, and M. Novák, *J. Electroanal. Chem.* **497**, 69 (2001).
- <sup>2</sup>S. Barazzouk, S. Hotchandani, and P. V. Kamat, *Adv. Mater. (Weinheim, Ger.)* **13**, 1614 (2001).
- <sup>3</sup>M. Csiszár, Á. Szűcs, M. Tölgyesi, J. B. Nagy, and M. Novák, *J. Electroanal. Chem.* **441**, 293 (1998).
- <sup>4</sup>C. Jehoulet, Y. S. Obeng, Y. T. Kim, F. Zhou, and A. J. Bard, *J. Am. Chem. Soc.* **114**, 4237 (1992).
- <sup>5</sup>L. O. Bulhões, Y. S. Obeng, and A. J. Bard, *Chem. Mater.* **5**, 110 (1993).
- <sup>6</sup>J. Chlistunoff, D. Cliffl, and A. J. Bard, *Thin Solid Films* **257**, 166 (1995).
- <sup>7</sup>L. R. Faulkner and Á. J. Bard, *Electrochemical Methods* (Wiley, New York, 1980).
- <sup>8</sup>M. S. Dresselhaus, G. Dresselhaus, and P. C. Eklund, *Science of Fullerenes and Carbon Nanotubes* (Academic, New York, 1996).
- <sup>9</sup>Q. Xie, E. Perez-Cordero, and L. Echegoyen, *J. Am. Chem. Soc.* **114**, 3978 (1992).
- <sup>10</sup>Á. Szűcs, M. Tölgyesi, M. Csiszár, J. B. Nagy, and M. Novák, *Electrochim. Acta* **44**, 613 (1998).
- <sup>11</sup>R. F. M. Lobo and C. A. C. Sequeira, *Nanotechnology* **17**, 4493 (2006).
- <sup>12</sup>R. F. Lobo and N. T. Silva, *Rev. Sci. Instrum.* **72**, 3505 (2001).
- <sup>13</sup>F. Wang, G. Dukovic, L. E. Brus, and T. F. Hein, *Phys. Rev. Lett.* **92**, 177401 (2004).
- <sup>14</sup>A. Hartschuh, H. N. Pedrosa, I. Novotny, and T. D. Krauss, *Science* **301**, 1354 (2003).
- <sup>15</sup>P. Janda, T. Krieg, and L. Dunsch, *Adv. Mater. (Weinheim, Ger.)* **10**, 1434 (1998).